Time-Synchronised Convolutional Perfectly Matched Layer for Improved Absorbing Performance in FDTD

Citation for published version:
Giannakis, I & Giannopoulos, A 2015, 'Time-Synchronised Convolutional Perfectly Matched Layer for Improved Absorbing Performance in FDTD', *IEEE Antennas and Wireless Propagation Letters*, vol. 14, pp. 690 - 693. https://doi.org/10.1109/LAWP.2014.2376981

Digital Object Identifier (DOI):
10.1109/LAWP.2014.2376981

Published In:
IEEE Antennas and Wireless Propagation Letters

Time-Synchronised Convolutional Perfectly Matched Layer for Improved Absorbing Performance in FDTD

Iraklis Giannakis and Antonios Giannopoulos

***Abstract*—A performance enhancing modification to the convolutional perfectly matched layer (CPML) technique for implementing the complex frequency shifted perfectly matched layer (CFS-PML) absorbing boundary condition is presented. By adopting this modification an apparent discrepancy in the time synchronisation between the CPML and the main FDTD algorithm is resolved. This is achieved by employing a semi-implicit approach which synchronises CPML with the main FDTD algorithm. It is shown through 2D and 3D numerical examples, that the suggested modification to the CPML algorithm increases its performance without increasing its computational cost.**

***Index Terms*—CFS-PML, CPML, FDTD, PML, RIPML, SC-PML.**

I. Introduction

PERECTLY matched layer (PML) first introduced in 1994 by [1], [2] and has since become the most used and well known absorbing boundary condition employed in finite-difference time-domain (FDTD) [3] electromagnetic modelling codes **as well as other numerical approaches like finite-element time-domain method [4]**. Different approaches for implementing PML in FDTD grids have been suggested which can be roughly categorised into: split field formulations [1], stretched coordinate PMLs (SC-PML) [2] and uniaxial perfectly matched layer (UPML) [5]. The SC-PML is considered possibly as the most attractive choice for implementing PML for a lot of reasons. Amongst them the most important are: that it makes the understanding of PML easier [6], it is easier to incorporate it in cylindrical and spherical coordinate systems [7], through SC-PML more elegant implementations can be obtained with which the PML is incorporated as a correction term [8], [9], dispersive and lossy media can be trivially treated [10] and finally it makes the implementation of complex frequency shifted PML (CFS-PML) more computationally efficient [11].

The CFS-PML was first introduced by [12] and has been proven [13] that can be used in order to reduce the late time reflections which occur when using SC-PML [14]. It has been also shown that CFS-PML decreases the numerical reflections related with the over-absorption of the propagating evanescent waves inside the PML region [15], [16], [17].

In [11] an elegant and computationally efficient way to implement CFS-PML has been introduced. This method is based on an SC-PML formulation and is referred to as the convolutional perfectly matched layer (CPML). CPML uses a recursive convolution approach first introduced by [18] (aimed for implementing dispersive media in FDTD) to evaluate the convolution between the complex frequency shifted stretching function and the spatial derivatives of the magnetic and the electric fields. An alternative interpretation of CPML based on an auxiliary differential equation (ADE) formulation is presented in [19], both of them result to the same equations.

Different methods for evaluating a convolution recursively have been suggested since the first recursive convolution (RC) [18] method was proposed. Piecewise linear recursive convolution (PLRC) [20] and trapezoidal recursive convolution [21] are considered second order accurate algorithms [21] and have been proven more accurate with respect to RC for both dispersive media [20] and PML [8] implementations. In contrast to standard RC, as introduced for modelling dispersive media, in CPML a TRC approach is employed by default. This is a result of convolving spatial derivatives that are at half a time step apart from the corresponding fields that are being updated by the FDTD equations. Therefore, CPML rivals other second order accurate techniques based on recursive integration [8], bilinear transform [22] and Z-transform [23].

It has been shown however, that in some examples CPML does not perform as well as other second order PML methods [8]. A closer inspection of the algorithm reveals that this is not due to the order of accuracy of the numerically evaluated convolution, but due to the fact that the implemented CFS-PML by the CPML is not properly synchronized with the main FDTD algorithm. In this work a simple semi-implicit scheme is proposed which results to the synchronization of CPML with the main FDTD without increasing the computational cost. The effects of the proposed synchronization to the overall performance of CPML are shown through 2D and 3D numerical examples.

II. Semi-Implicit CPML

Maxwell's equations (in frequency domain) using CFS-PML can be written in the general form as

$$j\omega\vec{D}_\omega = \nabla_s \times \vec{H}_\omega \tag{1}$$

$$j\omega\vec{B}_\omega = -\nabla_s \times \vec{E}_\omega \tag{2}$$

$$\nabla_s = \frac{1}{s_x}\frac{\partial}{\partial x}\vec{x} + \frac{1}{s_y}\frac{\partial}{\partial y}\vec{y} + \frac{1}{s_z}\frac{\partial}{\partial z}\vec{z} \tag{3}$$

I. Giannakis and A. Giannopoulos are with the School of Engineering, The University of Edinburgh, The King's Buildings, EH9 3JL, UK (e-mail: I.Giannakis@ed.ac.uk, A.Giannopoulos@ed.ac.uk)

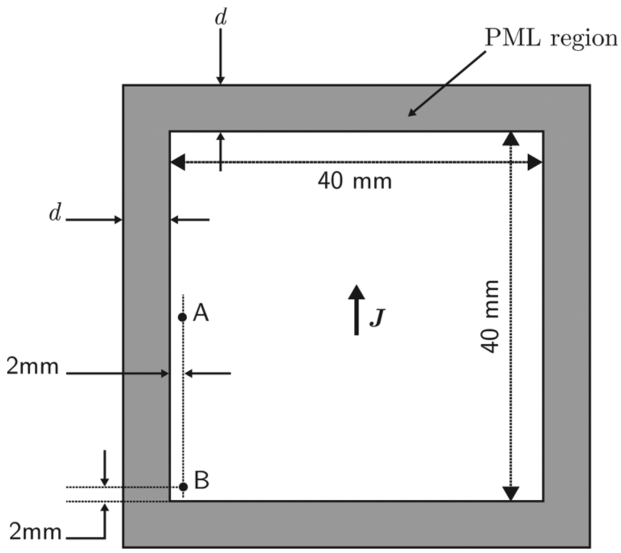

Fig. 1. A y-directed current source is located at the center of a 40×40 TE_z FDTD grid. The electric field E_y is probed at A and B points. The spatial step is $\Delta x = \Delta y = 1$ mm and the time step is 0.99 times the Courant limit. The thickness of the PML equals $d = 10$ mm [6].

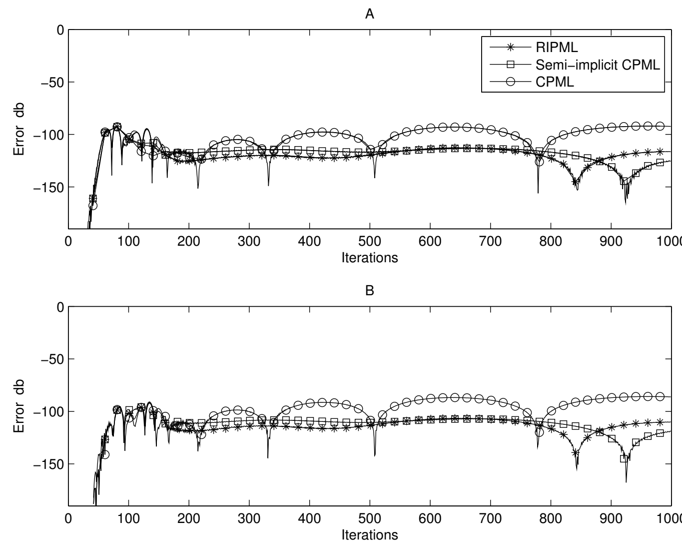

Fig. 2. Error calculated from (23) using CPML, RIPML and semi-implicit CPML. A and B corresponds to the receiving points illustrated in Fig. 1.

$$s_u = \kappa_u + \frac{\sigma_u}{\alpha_u + j\omega\epsilon_0} \tag{4}$$

where $\vec{E}$ is the electric field, $\vec{H}$ is the magnetic field strength, $\vec{B}$ is the magnetic field, $\vec{D}$ is the electric flux density, ω is the angular frequency, j is the imaginary unit $\left(j = \sqrt{-1}\right)$, $\nabla_s \times$ is the SC-PML curl operator, κ_u, σ_u and α_u are constants ($u \in \{x, y, z\}$) which define the complex frequency shifted stretching function proposed by [12] (4).

Transforming (1) and (2) to time domain results to

$$\frac{\partial \vec{D}}{\partial t} = \nabla_\kappa \times \vec{H} + \nabla_\zeta \times \vec{H} \tag{5}$$

$$\frac{\partial \vec{B}}{\partial t} = -\nabla_\kappa \times \vec{E} - \nabla_\zeta \times \vec{E} \tag{6}$$

$$\nabla_\kappa = \frac{1}{\kappa_x}\frac{\partial}{\partial x}\vec{x} + \frac{1}{\kappa_y}\frac{\partial}{\partial y}\vec{y} + \frac{1}{\kappa_z}\frac{\partial}{\partial z}\vec{z} \tag{7}$$

$$\nabla_\zeta = \zeta_x * \frac{\partial}{\partial x}\vec{x} + \zeta_y * \frac{\partial}{\partial y}\vec{y} + \zeta_z * \frac{\partial}{\partial z}\vec{z} \tag{8}$$

$$\zeta_u = -\frac{\sigma_u}{\epsilon_0 \kappa_u^2} e^{-\left(\frac{\sigma_u}{\epsilon_0 \kappa_u} + \frac{\alpha_u}{\epsilon_0}\right)t}. \tag{9}$$

For the case of D_x, following the procedure described in [11] yields

$$\begin{aligned}
&\delta_{\Delta t}\left(D^{n+1/2}_{x_{i+\frac{1}{2},j,k}}\right) = \\
&\frac{1}{k_y}\Lambda_{\Delta y}\left(H^{n+1/2}_{z_{i+\frac{1}{2},j,k}}\right) - \frac{1}{k_z}\Lambda_{\Delta z}\left(H^{n+1/2}_{y_{i+\frac{1}{2},j,k}}\right) \\
&+ \sum_{m=0}^{n}\left(Z^m_{0,y}\Lambda_{\Delta y}\left(H^{n-m+1/2}_{z_{i+\frac{1}{2},j,k}}\right) - Z^m_{0,z}\Lambda_{\Delta z}\left(H^{n-m+1/2}_{y_{i+\frac{1}{2},j,k}}\right)\right)
\end{aligned} \tag{10}$$

where $\delta_{\Delta t}$ is a second order in time central difference operator (11), $\Lambda_{\Delta u}$ is a spatial second order central difference operator (12), (13) and $Z^m_{0,u}$ is the discrete impulse response of ζ_u (14) [11].

$$\delta_{\Delta t}\left(F^t_{u_{i,j,k}}\right) = \frac{F^{t+\frac{\Delta t}{2}}_{u_{i,j,k}} - F^{t-\frac{\Delta t}{2}}_{u_{i,j,k}}}{\Delta t} \tag{11}$$

$$\Lambda_{\Delta z}\left(F^t_{u_{i,j,k}}\right) = \frac{F^t_{u_{i,j,k+\frac{1}{2}}} - F^t_{u_{i,j,k-\frac{1}{2}}}}{\Delta z} \tag{12}$$

$$\Lambda_{\Delta y}\left(F^t_{u_{i,j,k}}\right) = \frac{F^t_{u_{i,j+\frac{1}{2},k}} - F^t_{u_{i,j-\frac{1}{2},k}}}{\Delta y} \tag{13}$$

$$\begin{aligned}
Z^m_{0,u} &= \int_{m\Delta t}^{(m+1)\Delta t} \zeta_u(\tau)d\tau \\
&= -\frac{\sigma_u}{\epsilon_0\kappa_u^2}\int_{m\Delta t}^{(m+1)\Delta t} e^{-\left(\frac{\sigma_u}{\epsilon_0\kappa_u} + \frac{\alpha_u}{\epsilon_0}\right)\tau} d\tau \\
&= p_u e^{-\left(\frac{\sigma_u}{\kappa_u} + \alpha_u\right)\frac{m\Delta t}{\epsilon_0}}
\end{aligned} \tag{14}$$

$$p_u = \frac{\sigma_u}{\sigma_u\kappa_u + \kappa_u^2\alpha_u}\left(e^{-\left(\frac{\sigma_u}{\kappa_u} + \alpha_u\right)\frac{\Delta t}{\epsilon_0}} - 1\right). \tag{15}$$

The summation in (10) is calculated recursively by taking advantage of the exponential nature of Z_0 [18]. From (10) and (14) it is evident that the convolution in each time step takes place from 0 to $(n+1)\Delta t$. The spatial derivatives are assumed to be constant at the intervals $[n\Delta t,\ (n+1)\Delta t]$ and they are equal with the value they have at $(n+1/2)\Delta t$. This approach for evaluating recursively the convolution is known as TRC [21] which is more accurate compared with the first order RC suggested in [18] and rivals the accuracy [21] of PLRC [20]. The drawback of CPML is not the order of accuracy of TRC, but the fact that the approximated convolution is not synchronized with the main FDTD algorithm. This is evident in (10), in which the time derivative of the electric flux as well as the spatial derivatives of the magnetic field are evaluated at $(n + 1/2)\Delta t$ (using a second order approximation), while

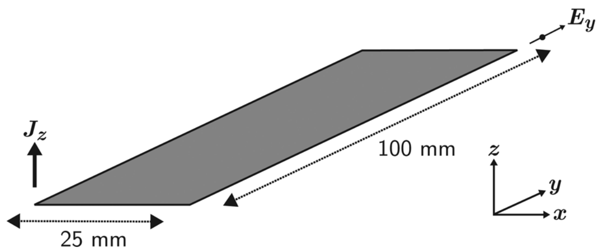

Fig. 3. A z-directed Hertzian dipole over a PEC plate. The spatial step is $\Delta x = \Delta y = \Delta z = 1$ mm and the time step is 0.99 times the Courant limit. The thickness of the PML equals $d = 10$ mm. E_y is monitored in the opposite corner of the source's location, one Yee cell away from the PEC plate [6].

the convolutions arising due to the presence of the PML are evaluated (using TRC which is a second oder approximation [21]) at $(n+1)\Delta t$.

From the above, Maxwell's equations using CPML are re-written in a discretized form using a second order accuracy in time scheme as

$$\frac{\partial \vec{D}}{\partial t}^{n+1/2} = \nabla_\kappa \times \vec{H}^{n+1/2} + \left(\nabla_\zeta \times \vec{H}\right)^{n+1} \tag{16}$$

$$\frac{\partial \vec{B}}{\partial t}^{n+1} = -\nabla_\kappa \times \vec{E}^{n+1} - \left(\nabla_\zeta \times \vec{E}\right)^{n+3/2}. \tag{17}$$

In order to synchronize $\nabla_\zeta \times \vec{H}$ and $\nabla_\zeta \times \vec{E}$ with the main FDTD algorithm in (16) and (17), a semi-implicit scheme is used in order to derive a second order approximation (in time) [6] of $\nabla_\zeta \times \vec{H}^{n+1/2}$ (18) and $\nabla_\zeta \times \vec{E}^{n+1}$ (19).

$$\nabla_\zeta \times \vec{H}^{n+1/2} \approx \frac{\nabla_\zeta \times \vec{H}^{n} + \nabla_\zeta \times \vec{H}^{n+1}}{2} \tag{18}$$

$$\nabla_\zeta \times \vec{E}^{n+1} \approx \frac{\nabla_\zeta \times \vec{E}^{n+1/2} + \nabla_\zeta \times \vec{E}^{n+3/2}}{2}. \tag{19}$$

Substituting (18) and (19) into (16) and (17) respectively, results into

$$\frac{\partial \vec{D}}{\partial t}^{n+1/2} = \nabla_\kappa \times \vec{H}^{n+1/2} + \frac{\left(\nabla_\zeta \times \vec{H}\right)^{n+1} + \left(\nabla_\zeta \times \vec{H}\right)^{n}}{2} \tag{20}$$

$$\frac{\partial \vec{B}}{\partial t}^{n+1} = -\nabla_\kappa \times \vec{E}^{n+1} - \frac{\left(\nabla_\zeta \times \vec{E}\right)^{n+3/2} + \left(\nabla_\zeta \times \vec{E}\right)^{n+1/2}}{2} \tag{21}$$

The modified CPML saves in temporary variables the values of $\nabla_\zeta \times \vec{H}^{n}$ and $\nabla_\zeta \times \vec{E}^{n+1/2}$ and subsequently calculates $\nabla_\zeta \times \vec{H}^{n+1}$ and $\nabla_\zeta \times \vec{E}^{n+3/2}$ according to [11]. The second order semi-implicit approximations in (18), (19) can now be trivially calculated and added as correction terms in the CPML-FDTD code. From the above it is evident that no additional variables are needed to be stored compared with CPML.

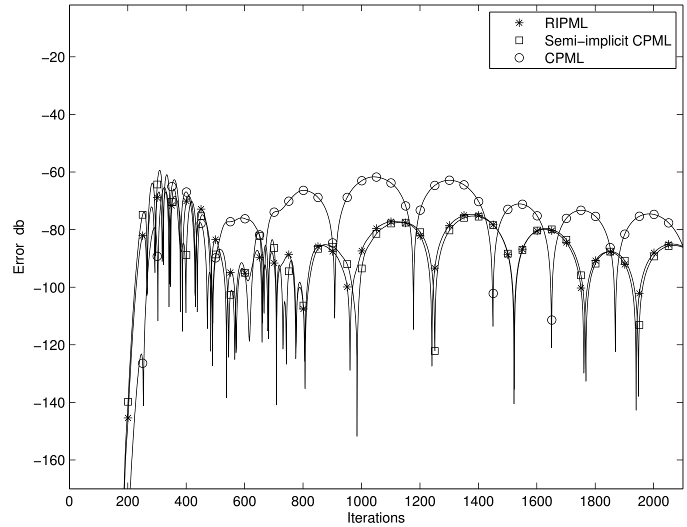

Fig. 4. Calculated error (23) using semi-implicit CPML, CPML and RIPML for the case study described in Fig. 3.

III. Numerical results

The performance of CPML with the proposed modification is validated through 2D and 3D numerical examples. The numerical experiments are similar to the ones used in [6] and [8]. The proposed algorithm i.e. semi-implicit CPML, is compared with the standard CPML in order to show how the suggested synchronization affects the overall performance of the implemented CFS-PML. Semi-implicit CPML is also compared with the recursive integration PML (RIPML), which, as it is shown in [8] achieves a small increase in performance with respect to CPML.

A. Current Source Radiating in an Unbounded Two-Dimensional Region

In the first example a TE_z (H_z, E_y, E_x) FDTD is employed. The dimensions of the model are 40×40, the discretization step equals to $\Delta x = \Delta y = 1$ mm (uniform along the grid) and the time step is 0.99 times the Courant limit. A current source is placed at the center of the grid and the time variation of the source is equal with [6]

$$I(t) = -2\frac{t - t_0}{t_w} e^{-\left(t - \frac{t_0}{t_w}\right)^2} \tag{22}$$

where $t_w = 26.53$ ps and $t_0 = 4t_w$. The electric field E_y is sampled at A and B points (see Fig. 1). The sampled E_y fields are compared to a reference solution and the error defined in (23) is calculated.

$$Error|_{i,j}^{n} = 20 \cdot \log_{10} \frac{||E|_{i,j}^{n} - E_{ref}|_{i,j}^{n}||}{E_{ref_{max}}|_{i,j}}. \tag{23}$$

Where $E|_{i,j}^{n}$ is the probed electrical field at grid points (i,j) and at n time step, $E_{ref}|_{i,j}^{n}$ is the reference solution and $E_{ref_{max}}|_{i,j}$ is the maximum absolute value of the reference solution.

The thickness of the PML is 10 Yee cells and the optimum value for σ_{max} is calculated according to [6]

$$\sigma_{max} = \frac{0.8(m+1)}{Z \cdot dl} \tag{24}$$

where Z is the impedance of the medium, dl is the discretization step and $m = 3$ is the order of the polynomial function which is used to scale σ_u along the PML [6]. A constant value $\kappa_u = 1$ is applied along the FDTD. An inverse linear scaling is applied to α_u [6] with $\alpha_{max} = 0.2$. Fig. 2 illustrates the error at the receiving points A and B (see Fig. 1) using CPML, RIPML and the semi-implicit CPML method. It is evident that there is an improvement in accuracy using semi-implicit CPML and RIPML compared with CPML. The differences regarding the accuracy between RIPML and semi-implicit CPML are negligible. The main advantage of this new semi-implicit CPML formulation is the simplicity in implementing it into existing CPML codes.

B. Current Source Over a Thin Perfect Electrical Conductor (PEC) Plate in a Three-Dimensional Domain

In the second example the performance of the modified CPML when evanescent waves occur is examined. The dimensions of the 3D domain are $31 \times 106 \times 6$, the discretization step is uniform along the domain and equals to $\Delta x = \Delta y = \Delta z = 1$ mm and the time step is 0.99 times the Courant limit. A $z-$directed Hertzian dipole is placed on top of the edge of a 25×100 mm PEC plate [8]. The time evolution of the current source is given by (22) with $t_w = 53$ ps and $t_0 = 4t_w$ [8]. The width of the PML is 10 Yee cells. The E_y field is probed at the opposite corner from the source's location, 1 mm away from the PEC plate (see Fig. 3). The values of the stretching function are $\kappa_u = 1$ (constant along the PML), σ_{max} is given by (24) with $m = 3$. A linear function is used to express α_u with $\alpha_{max} = 0.24$. Fig. 4 illustrates the error defined in (23) using CPML, semi-implicit CPML and RIPML. It is evident that synchronization increases the overall performance of CPML. Again semi-implicit CPML and RIPML exhibit negligible differences in performance.

IV. Conclusions

Small differences in time synchronisation between the main FDTD and the CPML algorithm have an impact on the overall performance of PML absorbing boundary condition. A simple approach is suggested which resolves these performance issues by using a second order semi-implicit approximation. The proposed modification can be implemented in a straightforward manner as a correction in a CPML-FDTD code. Numerical examples in 2D and 3D domains demonstrate the improvement in performance that can be achieved using the modified CPML over the original implementation.

Acknowledgment

The authors would like to acknowledge the financial support of the UK Engineering and Physical Sciences Research Council (EPSRC) and Defence Science and Technology Laboratory (Dstl).

References

[1] J. P. Berenger, "A perfectly matched layer for the absorption of electromagnetic waves," *J. Comput. Phys.,* vol. 114 pp. 185-200, 1994.

[2] W. C. Chew and W. H. Weedon, "A 3-D perfectly matched medium form modified Maxwell's equations with streched coordinates," *IEEE Microw. Opt. Technol. Lett.,* vol. 7, no. 13, pp. 599-604, Sep. 1994.

[3] K. Yee, "Numerical solution of initial boundary value problems involving Maxwell's equations in isotropic media," *IEEE Trans. Antennas Propag.*, vol. 14, no. 3, pp. 302-307, May 1966.

[4] S. Wang, R. Lee, and F.L. Teixeira, "Anisotropic-Medium PML for Vector FETD with Modified Basis Functions?, IEEE Trans. Antennas Propagation, vol. 54, no. 1, pp. 20-27, Jan. 2006.

[5] S. D. Gedney, "An anisotropic perfectly matched layer-absorbing medium for the truncation of FDTD lattices," *IEEE Trans. Antennas Propag.*, vol. 44, no. 12, pp. 1630-1639, Dec. 1996.

[6] A. Taflove and S. C. Hagness, *Computational Electrodynamics: The Finite-Difference Time-Domain Method*, 3rd ed. Boston, MA: Artech House, 2005.

[7] F. L. Teixeira and W. C. Chew, "PML-FDTD in cylindrical and spherical coordinates," *IEEE Microw. Guided Wave lett.,* vol 43, pp. 1460-1463, Aug. 1995.

[8] A. Giannopoulos, "An improved new implementation of complex frequency shifted PML for the FDTD method," *IEEE Trans. Antennas Propag.*, vol. 56, no. 9, pp. 2995-3000, Sep. 2008.

[9] F. H. Drossaert and A. Giannopoulos, "A non-split complex frequnecy-shifted PML based on recursive integration for FDTD modeling of elastic waves," *Geophysics*, vol. 72, no. 2, pp. T9-T17, Apr. 2007.

[10] S. A. Cummer, "A simple, nearly perfectly matched layer for general electromagnetic media," *IEEE Microw. and Wireless Comp. Lett.*, vol. 13, no. 3, pp. 128-130, Mar. 2003.

[11] J. Roden and S. Gedney, "Convolution PML (CPML): an efficient FDTD implementation of the CFS-PML for arbitrarily media," *Microw. Opt. Technol. Lett.,* vol. 27, pp. 334-339, Dec. 2000.

[12] M. Kuzuoglu, R. Mittra, "Frequency dependence of the constitutive parameters of causal perfectly matched anisotropic absorbers," *IEEE Microw. Guided Wave Lett.*, vol. 6, no. 12, pp. 447-449, Dec. 1996.

[13] E. Becache, P. G. Petropoulos and S. D. Gedney, "On the long-time behavior of unsplit perfectly matched layers," *IEEE Trans. Antennas Propag.*, vol. 52, no. 5, pp. 1335-1342, May 2004.

[14] S. Abarbanel, D. Gottlieb and J. S. Hesthaven, "Long time behavior of the perfectly matched layer equations in computational electromagnetics," *J. Scientif. Comput.*, vol. 17, no. 14, pp. 405-422, Dec. 2002.

[15] J. P. Berenger, "Evanescent waves in PML's: origin of the numerical reflection in wave-structure interaction problems," *IEEE Trans. Antennas Propag.*, vol. 47, no. 10, pp. 1497-1503, Oct. 1999.

[16] J. P. Berenger, "Numerical reflection of evanescent waves by PMLs: origin and interpretation in the FDTD case, expected consequences to other finite methods," *Int. J. Numer. Modelling Elect. Networks Devices Fields*, vol. 13, pp. 103-114, Mar. 2000.

[17] J. P. Berenger, *Perfectly Matched Layer (PML) for Computational Electromagnetics*, 1st edition, Morgan and Claypool publishers, 2007.

[18] R. J. Luebbers, F. Hunsberger, K. S. Kunz, R. B. Standler and M. Schneider, "A frequency-dependent finite-difference time-domain formulation for dispersive media using FDTD," *IEEE Trans. Antennas Propag.,* vol. 44, no. 6, pp. 792-797, Jun. 1996.

[19] S. Gedney and B. Zhao, "An auxiliary differential equation formulation for the complex-frequency shifted PML," *IEEE Trans. Antenn. Propag.*, vol. 58, no. 3 pp. 838-847, Mar. 2010.

[20] D. F. Kelley and R. J. Luebbers, "Piecewise linear recursive convolution for dispersive media using FDTD," *IEEE Trans. Antennas Propag.*, vol. 44, no. 6, pp. 792-797, Jun. 1996.

[21] R. Siushansian and J. L. Vetri, "Efficient evaluation of convolution integrals arising in FDTD formulations of electromagnetic dispersive media," *J. Electromag. Waves Applicat.*, vol. 11, no. 1, pp. 101-117, 1997.

[22] X. Zhuansun and X. Ma, "Bilinear transform implementation of the SC-PML for general media and general FDTD schemes," *IEEE Trans. Electrom. Compatib.*, vol. 54, no. 2, pp. 343-350, Apr. 2012.

[23] J. Li and J. Dai, "Z-Transform implementation of the CFS-PML for arbitrary media," *IEEE Microw. Comp. Lett.*, vol. 16, no. 8, pp. 437-439, Aug. 2006.